

JET NOISE REDUCTION BY FLUIDIC INJECTION FROM A ROTATING PLUG

M. Koenig

Acoustics Department
SNECMA, SAFRAN Group
Moissy-Cramayel, FRANCE
maxime.koenig@etu.univ-poitiers.fr

C. Fourment-Cazenave, P. Jordan, Y. Gervais

Département Fluides, Thermique et Combustion
Institut Pprime
CEAT, Poitiers, FRANCE
carine.fourment@univ-poitiers.fr, peter.jordan@univ-poitiers.fr, yves.gervais@univ-poitiers.fr

ABSTRACT

We explore a novel jet noise reduction device involving the steady injection of fluid from two diametrically-opposed ports on a rotating centerbody. For the rotation speeds currently possible, noise reductions are observed over a low-frequency range, up to the rotation frequency. Preliminary results suggest that the noise reduction mechanism may be due to the most unstable flow modes (axisymmetric mode $m = 0$) being deprived of fluctuation energy due to an excitation of less unstable modes (azimuthal mode $m = 2$ driven at $St = 0.23$).

INTRODUCTION

Jet noise control is most often effected by means of either geometric nozzle modifications (Loheac *et al.* (2004), Samimy *et al.* (1993), Zaman *et al.* (2003)), steady or unsteady fluidic injection (Laurendeau *et al.* (2008), Castelain *et al.* (2008), Arakeri *et al.* (2003), Maury *et al.* (2011)) and plasma discharge (Samimy *et al.* (2007)). In all of these cases perturbations are introduced in the vicinity of the nozzle lip, and in the unsteady cases by means of a localised pulsation or injection modulation. In this study we propose an alternative actuation, fluidic perturbations being introduced in the central region of the jet by means of steady injection from a rotating plug; thus we have unsteadiness, but no pulsation.

The device is tested on a round jet with Mach number, $M = 0.3$, Reynolds number, $Re = 3.10^5$, and low frequency noise reductions are observed up to the rotation frequency. Analysis of the acoustic and flow measurements (performed by means of stereoscopic, time-resolved PIV) show that for the acoustically beneficial actuation the fluctuation energy of the axisymmetric mode of the flow—which is known to be acoustically important, dominating the sound field at low emission angles—is reduced. This appears to be due to its being deprived of energy on account of the excitation of mode

$m = 2$, which is less unstable than the axisymmetric mode at the acoustically-effective excitation frequency; this observation is based on a linear stability analysis (Michalke (1971)) of the mean-velocity profile just downstream of the centerbody.

EXPERIMENTAL SETUP

The experiments were performed in the anechoic jet noise facility, “Bruit et Vent” (Noise and Wind), of the CEAT, Poitiers. A Mach 0.3 cold jet is studied in this paper (this being due to limitations in the rotation speeds of the actuator). The jet diameter is equal to 0.05 m. A 0.03 m diameter plug (centerbody) is mounted in the centre of the jet (see figure 1), and is driven in rotation by an electric motor. Air is injected into the plug via a hole in the crankshaft.¹ The air is ejected at 240 m/s into the main jet by two 0.0013 m diameter, diametrically opposed, control ports. The control-jet flow rate is less than 0.5% that of the main jet.

Microphone measurements were made at 30 diameters from the jet, at downstream angles of 20° and 30°. A moving average was used to smooth the spectra, and peaks associated with sound radiated by the electric motor have been removed by a notch filter in the results presented here.

The jet flow velocity was measured by a LaVision time-resolved Stereo-PIV system using a camera with 1024x1024 pixel resolution. The light source was a 10 mJ Quantronix Darwin duo laser (light sheet thickness 2 mm) and the flow was seeded with oil smoke. Three components of velocity were measured in $r - \theta$ planes at a range of axial stations by two SA1 Photron cameras. The sampling frequency was 2.7kHz. 10000 PIV image pairs were recorded, this being sufficient for convergence of first and second order statistics. Data-processing consisted of a five-pass correlation routine with 64x64 pixel correlation for the first pass, 16x16 pixel for

¹The crankshaft looks like a piece of bucatini.

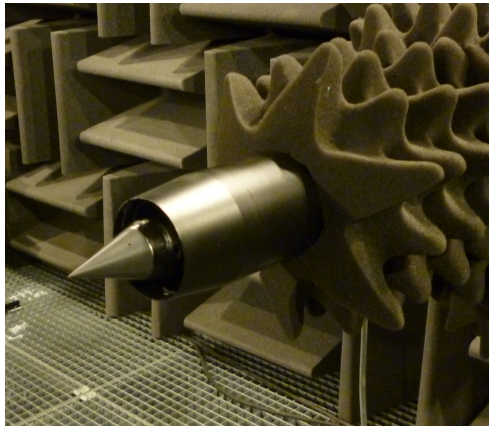


Figure 1: Rotating plug actuator in “Bruit et Vent”.

the final pass and with a 50% correlation overlap at each pass. The spatial resolution was one velocity vector every 0.75 mm for the small window size (near the jet exit) and one velocity vector every 1.5 mm for the large window size (around the end of the potential core).

Flow fields are analysed for the baseline jet and for jets perturbed by fluidic injection from plugs rotating at $St = 0.06$ (150Hz), $St = 0.12$ (300Hz) and $St = 0.23$ (600Hz). The exit Mach number of the main jet is $M = 0.3$. At the time of this conference, from a total of 17 axial measurement planes, data from three ($x/D = 2.5$, $x/D = 3$ and $x/D = 6$) is available and will be presented in what follows.

ACOUSTIC RESULTS

Figure 2 shows results for three different rotation frequencies at a fixed injection flow-rate. We see that, aside from the high-frequency self-noise of the actuator ($St > 1.5$)², no difference is observed between the uncontrolled and controlled flows at $St_{0.06}$ (green dashed line): the actuator does not here produce any change in the flow as far as its low-frequency sound producing dynamics are concerned. The first response of the jet source dynamics to actuation occurs at $St_{0.12}$: the jet is now louder (red dashed line); the change from green line to red line in figure 2 occurs abruptly at a rotation frequency of $St_{0.12}$, indicating a sudden bifurcation of the jet from its baseline equilibrium state to a new louder equilibrium state. The blue dotted line (rotation frequency of $St_{0.23}$) shows a case where a benefit has been produced at low frequency, and figure 2 (Bottom) shows the evolution between red dashed line and blue dotted line in figure 2 (Top): once the “new” equilibrium state has been provoked, the response of the jet to actuation frequency is smooth, noise reduction being achieved over a progressively broader frequency range as rotation frequency is increased.

²The high-frequency noise increase is believed to be associated with scattering, by the plug, of turbulence associated with the fluidic injection: we have established that this component of the noise has a lower velocity scaling than main jet noise, which means that at higher Mach numbers the high frequency penalty is less severe; preliminary measurements at higher Mach number (Mach 0.6) confirm this.

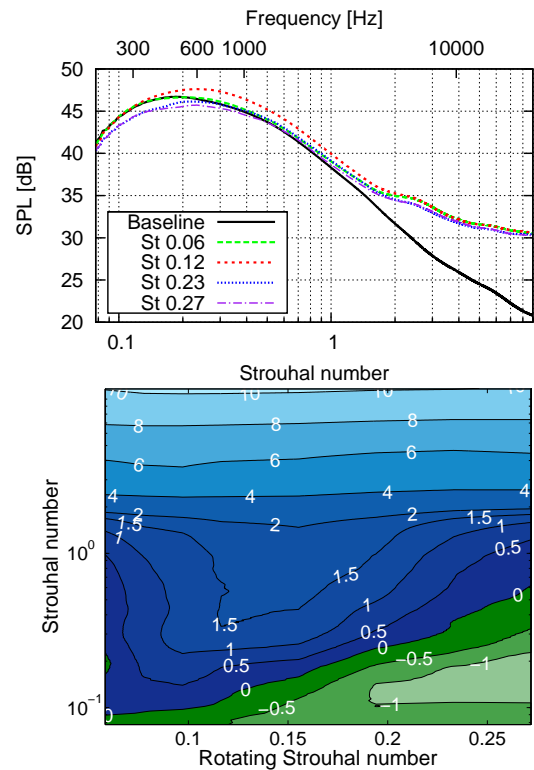


Figure 2: Top: baseline and controlled noise spectra at 20° and Mach 0.3, $U_{microjet} = 240\text{m/s}$, rotating frequencies are $St_{0.06}$, $St_{0.12}$ and $St_{0.23}$; bottom: change in noise (contours in dB) as a function of rotation frequency and Strouhal number.

It is interesting to note that: (1) below a certain frequency (rotation rate corresponding to the green dashed line in figure 2), the jet is insensitive to actuation as far as the low-frequency sound sources are concerned; (2) once we change the equilibrium state of the flow, from that producing the green dashed line sound spectrum to that producing the red dashed line sound spectrum in figure 2, we have a flow with a greater sensitivity to control (in terms of the sound-producing dynamics). Figure 2 furthermore shows that the increase in cross-over frequency (between noise reduction and noise increase) is proportional to the increase in rotation frequency for the range possible with our current actuator. This trend suggests that with higher rotation rates reductions over a broader frequency range will be possible; a new actuator, capable of higher rotation rates, is being developed to this end.

AERODYNAMIC RESULTS

In this section we examine the structure of the flow field in terms of its first and second order statistical moments, and its azimuthal modal structure. At this stage the analysis is effected in the context of a Reynolds decomposition of the velocity field; the analysis is to be repeated in the context of a triple decomposition, such as done by Hussain & Reynolds (1970).

Statistical moments

The impact of the fluidic actuation on the first and second order statistical moments of the velocity field is summarised in figures 3 through 7 for the three axial measurement planes for which data is presently available. In the near-plug region the axial velocity field is reduced by the actuation in regions of peak velocity, an increase being observed on the centerline, just downstream of the plug tip. In the downstream region, at $x/D = 6$, it can be seen how the global effect comprises a greater spreading of the jet (cf. figure 4). It is also worth pointing out that as the rotation frequency is increased from $St_{0.06}$ to $St_{0.12}$ and then to $St_{0.23}$, the evolution of the structure of the mean axial velocity field in the downstream region is, like the evolution of the sound field, not monotonic: the smallest meanfield defect results from the $St_{0.06}$ rotation (recall that no change in low-frequency noise is observed for this case), the largest for the $St_{0.12}$ rotation (which corresponds to a LF noise increase), while the $St_{0.23}$ rotation (with which there is associated a LF noise decrease) lies between the two. In the near-plug region the defect in the axial component of the mean field is more monotonic, the mean velocity increasing progressively in the plug wake. Where the mean radial velocity is concerned the changes are slight.

The most intriguing change in the mean field is manifest in the azimuthal component: the amplitude of this double-S in the near-plug region is monotonic as rotation speed is increased. The mechanism responsible is not clear at present; two possible explanations are: (1) each of the control jets induces a system of four radially-aligned counter-rotating vortices: if we compare with the example of a jet in cross-flow (Kelso *et al.* (1996) for example), these may be due to the so-called ‘wall’ vortices shed from the base of the control jet, and the counter-rotating vortex pair generally observed in the vicinity of the trajectory of the wall jet after it has become parallel to the main flow; (2) the defect is associated with changes in the Reynolds stress tensor. A triple decomposition (by which the Reynolds stress tensor can be decomposed into phase-averaged, background and mixed terms) and feature extraction algorithms will later be used to help establish which, if either, of these hypotheses is consistent with both the data and the flow equations.

The Reynolds stresses are shown in figures 5 through 6, and a summary of the change in the region of peak stress is shown by the histogram in figure 7. Of interest is the fact that the $St_{0.23}$ case, while it produces considerable increases in the near-nozzle region, is the configuration that makes the smallest change in the downstream region ($x/D = 6$). Also, the peak shear stresses, $u_\theta u_\theta$, $u_x u_\theta$ and $u_r u_\theta$, they all participate in the mean radial and azimuthal momentum balance, show drastic changes with increasing frequency, as does the corresponding mean velocity (cf. equation below). Again, triple-decomposition will allow this question to be further probed.

$$\begin{aligned} \rho_0 \left(\overline{u_x} \frac{\partial \overline{u_x}}{\partial x} + \overline{u_r} \frac{\partial \overline{u_x}}{\partial r} \right) &= \frac{\partial \overline{P}}{\partial x} + \mu \overline{\delta_x} - \rho_0 \left(\frac{\partial \overline{u_x^2}}{\partial x} + \frac{1}{r} \frac{\partial r \overline{u_x' u_r'}}{\partial r} \right) \\ \rho_0 \left(\overline{u_x} \frac{\partial \overline{u_r}}{\partial x} + \overline{u_r} \frac{\partial \overline{u_r}}{\partial r} - \frac{\overline{u_\theta^2}}{r} \right) &= \frac{\partial \overline{P}}{\partial r} + \mu \overline{\delta_r} - \rho_0 \left(\frac{\partial \overline{u_r^2}}{\partial x} + \frac{1}{r} \frac{\partial r \overline{u_r'^2}}{\partial r} - \frac{\overline{u_\theta^2}}{r} \right) \\ \rho_0 \left(\overline{u_x} \frac{\partial \overline{u_\theta}}{\partial x} + \overline{u_r} \frac{\partial \overline{u_\theta}}{\partial r} + \frac{\overline{u_\theta} \overline{u_r}}{r} \right) &= \mu \overline{\delta_\theta} - \rho_0 \left(\frac{\partial \overline{u_x' u_\theta'}}{\partial x} + \frac{1}{r} \frac{\partial r \overline{u_r' u_\theta'}}{\partial r} + \frac{\overline{u_r' u_\theta'}}{r} \right) \end{aligned}$$

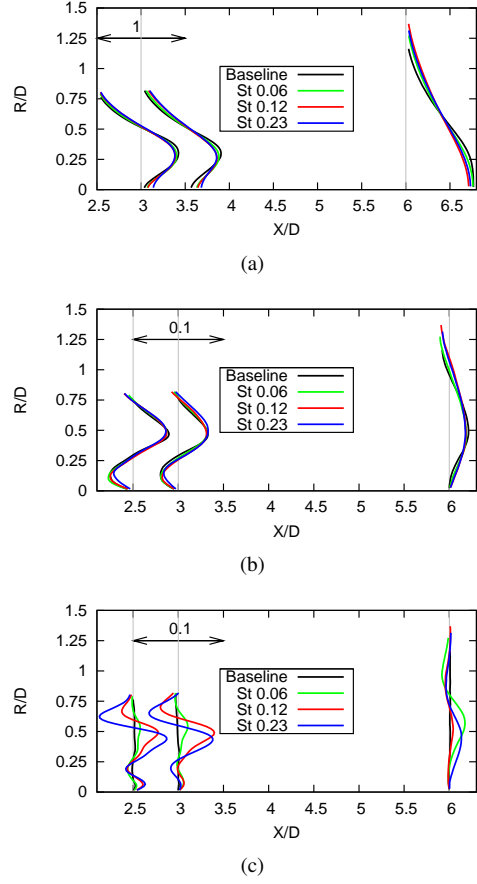


Figure 3: Mean components of the velocity vector: (a) Axial velocity $\langle U_x \rangle / U_j$; (b) Radial velocity $\langle U_r \rangle / U_j$; (c) Azimuthal velocity $\langle U_\theta \rangle / U_j$.

Azimuthal modal structure

The three components of the velocity field are expanded in a Fourier series decomposition and the results summarised by means of the histograms shown in figures 8, 9 and 10, which, while they represent only the peak radial values are broadly representative of the overall (radially-integrated) levels. Due to space limitations these figures cannot be discussed exhaustively, and we therefore focus on a number of interesting features, which may also be pertinent with regard to the changes in radiated sound: in the near nozzle region, the $St_{0.23}$ actuation produces very high fluctuation levels in mode $m = 2$ of the *radial and azimuthal* velocity components. In the downstream region the axisymmetric component of the flow driven by the $St_{0.23}$ actuation has undergone, with respect to the baseline case, a reduction in fluctuation energy of its axial and radial components, while its axisymmetric azimuthal fluctuations are slightly increased. As the noise reduction at low emission angles occurs in the vicinity of the spectral peak, which is known to be dominated by the axisymmetric mode, and which some recent analysis suggests is predominantly driven by axially-coherent, axisymmetric wavepacket structures (cf. Cavalieri *et al.* (2011a,2011b,2011c)), we can postulate that this reduction in the fluctuation energy of the ax-

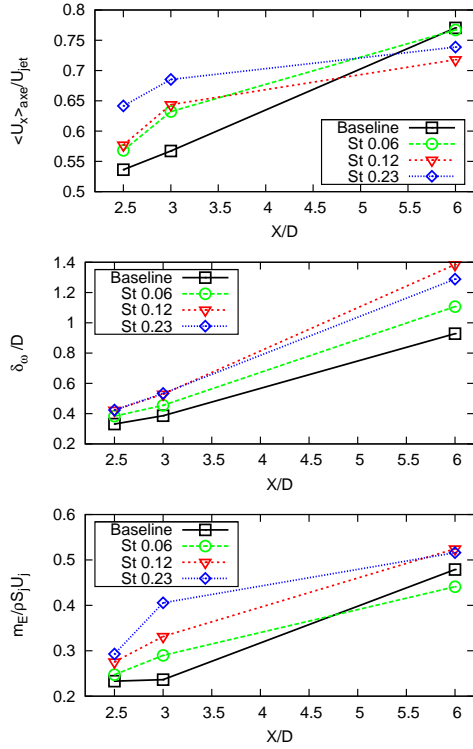


Figure 4: Axial evolution of: axial mean velocity on the centerline (top); vorticity thickness (middle); entrainment (bottom)

isymmetric component of the axial and radial velocity fluctuations (topology corresponding to convection of vortical-ring-like structures), corresponds to a reduction in the fluctuation energy of the said, acoustically-effective, wavepackets, and is thus one of the reasons for the noise reduction.

Our working hypothesis regarding this change in the axisymmetric component of the fluctuating velocity field is based on some preliminary linear stability calculations (Cavaliere (2011d)) using an experimental velocity profile in the near nozzle region, and on the results of phase-averaged measurements (not shown): in the near-nozzle region, for mode $m = 2$, $St_{0.06}$ and $St_{0.12}$ are close to the most unstable frequencies, whereas $St_{0.23}$ is considerably less unstable; in addition to this, phase-averaged measurements at $St_{0.06}$ and $St_{0.12}$ show the response of the jet to comprise highly organised, convected waves with global synchronisation, while the response at $St_{0.23}$ does not show such an organised, eigen-like response. These observations lead us to hypothesise that the increased effectiveness of the device as the frequency is increased is due to the fact that we progressively draw the fluctuation energy of the flow into motions that are less unstable, thereby stifling the acoustically-important axisymmetric fluctuating motions of the flow.

CONCLUSION AND PERSPECTIVE

The jet noise control device explored in this paper produces flow mechanisms that are quite different to those produced by other fluidic devices, and noise reductions are

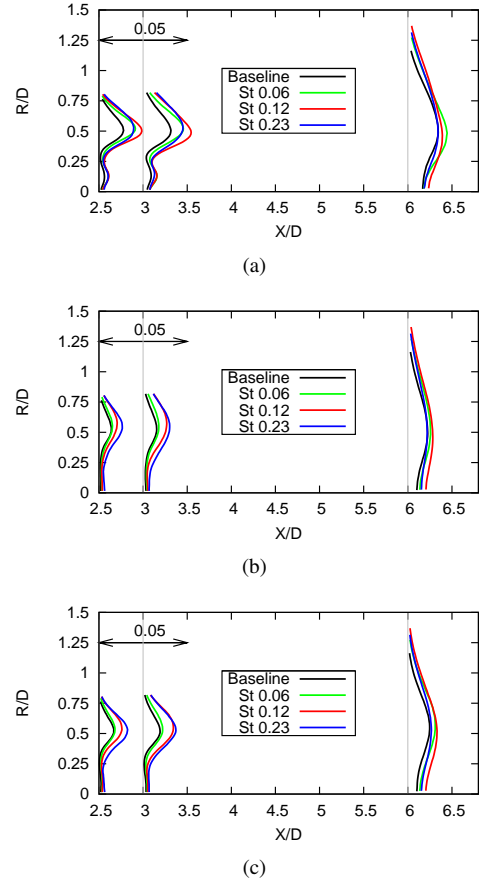


Figure 5: Diagonal components of the Reynolds stress tensor: (a) $\langle u_x^2 \rangle / U_j^2$; (b) $\langle u_r^2 \rangle / U_j^2$; (c) $\langle u_\theta^2 \rangle / U_j^2$.

achieved with considerably lower injection flow-rates. Also, much of the fluctuation energy is introduced into the flow via centerbody rotation rather than injection modulation or pulsation. The current working hypothesis with regard to the noise-reduction effectiveness of the device is that by exciting flow modes with low instability, the most unstable flow modes in the potential core region, which are also the most acoustically-efficient, are deprived of fluctuation energy and thus generate less sound.

ACKNOWLEDGEMENTS

The present work was supported by SNECMA. The authors would also like to thank Patrick Braud for his contribution to the experiments, and André Cavaliere for helpful discussions and for some preliminary stability calculations that he performed.

REFERENCES

Arakeri, V.H., Krothapalli, A., Siddavaram, V., Alkisar, M.B. and Lourenco, L.M., 2003 "On the use of microjets to suppress turbulence in a Mach 0.9 axisymmetric jet", Journal of Fluid Mechanics, Vol. 490, pp 75-98.

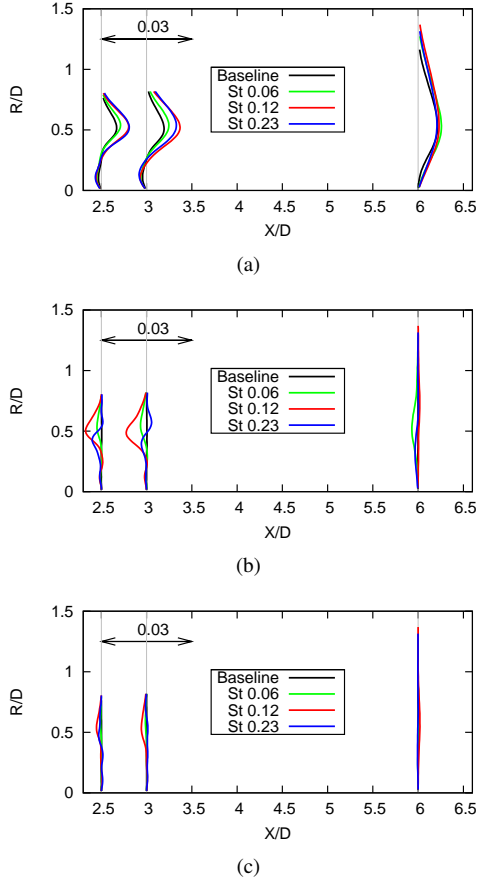


Figure 6: Off-diagonal components of the Reynolds stress tensor: (a) $\langle u'_x u'_r \rangle / U_j^2$; (b) $\langle u'_x u'_\theta \rangle / U_j^2$; (c) $\langle u'_r u'_\theta \rangle / U_j^2$.

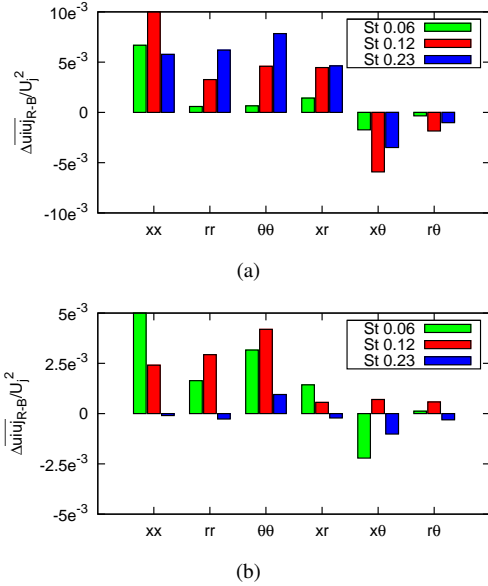


Figure 7: Changes in the region of peak Reynolds stresses relatively to the baseline: (a) $X = 2.5D$ (b) $X = 6D$.

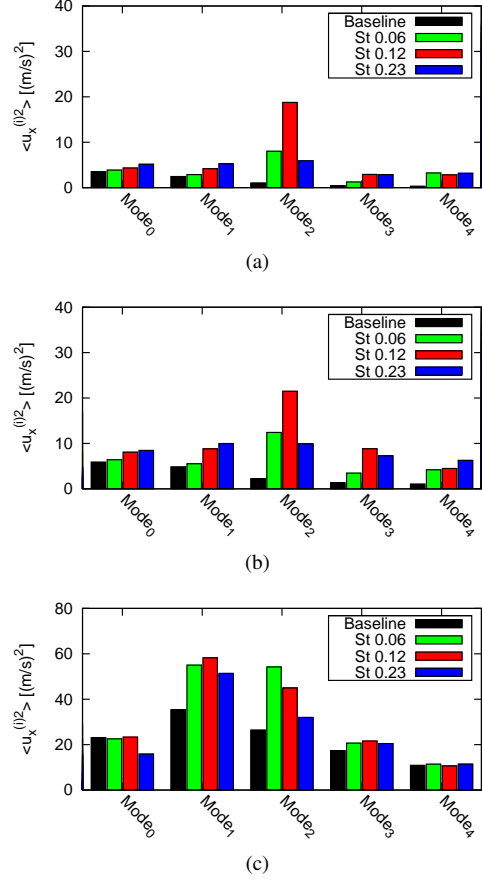


Figure 8: Fluctuation energy of azimuthal modes of axial velocity component at $R=0.25D$ (where peak levels are observed); (a) $x/D = 2.5$; (b) $x/D = 3$; (c) $x/D = 6$.

Castelain, T., Sunyach, M., Juvé, D. and Béra, J.-C., 2008 "Jet-noise reduction by impinging microjets: an acoustic investigation testing microjet parameters", *AIAA Journal*, Vol. 46, No. 5, pp. 1081-1087.

Cavalieri, A.V.G., Daviller, G., Comte, P., Jordan, P., Tadmor, G. and Gervais, Y., 2011a "Using large eddy simulation to explore sound-source mechanisms in jets", *to appear in Journal of Sound and Vibration*.

Cavalieri, A.V.G., Jordan P., Agarwal A. and Gervais Y., 2011b "Jittering wave-packet models for subsonic jet noise", *to appear in Journal of Sound and Vibration*.

Cavalieri, A.V.G., Rodriguez, D., Jordan, P., Colonius, T. and Gervais, Y., 2011c "Inlet conditions and wave-packets in subsonic jet noise" 7th International Symposium on Turbulence and Shear Flow Phenomena, Ottawa, Canada.

Cavalieri, A.V.G., 2011d private communication on preliminary linear stability equations.

Hussain, A.K.M.F. and Reynolds, W.C., 1970 "The mechanics of an organized wave in turbulent shear flow", *Journal of Fluid Mechanics*, Vol. 41, pp. 241-258.

Kelso, R.M., Lim, T.T. and Perry, A.E., 1996 "An experimental study of round jets in cross-flow", *Journal of Fluid*

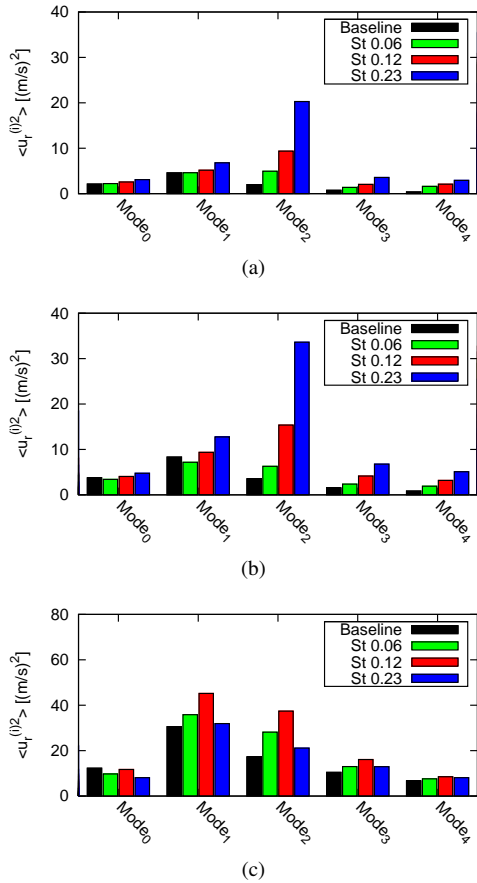


Figure 9: Fluctuation energy of azimuthal modes of radial velocity component at $R=0.25D$ (where peak levels are observed); (a) $x/D = 2.5$; (b) $x/D = 3$; (c) $x/D = 6$.

Mechanics, Vol. 306, pp. 111-144.

Laurendeau, E., Jordan, P., Bonnet, J.P., Delville, J., Parnoudeau, P. and Lamballais, E., 2008 “Subsonic jet noise reduction by fluidic control : the interaction region and the global effect”, *Physics of Fluids*, Vol. 20, pp. 1- 15.

Loheac, P., Julliard, J. and Dravet, A., 2004 “CFM56 jet noise reduction with the chevron nozzle”, Proceedings 2004-3044, 10th AIAA/CEAS Aeroacoustics Conference, Manchester, United Kingdom.

Maury, R., Cavalieri, A.V.G., Jordan, P., Delville, J. and Bonnet, J.-P., 2011 “Jet noise reduction using pulsed fluidic actuation”, 7th International Symposium on Turbulence and Shear Flow Phenomena, Ottawa, Canada.

Michalke, A., 1971 “Instabilität eines Kompressiblen

Runden Freistrahls unter Berücksichtigung des Einflusses der Strahlgrenzschichtdicke” *Z. Flugwiss*, Vol. 19, pp 319-328; English translation: NASA TM 75190, 1977.

Samimy, M., Zaman, K. and Reeder, M., 1993 “Effect of tabs on the flow and noise field of an axisymmetric jet”, *AIAA Journal*, Vol. 31, No. 4.

Samimy, M., Kim, J.-H., Kastner, J., Adamovich, I. and Utkin, Y., 2007 “Active control of a Mach 0.9 jet for noise mitigation using plasma actuators”, *AIAA Journal*, Vol. 45, No. 4., pp 890-901.

Zaman, K., Wang, F. and Georgiadis, N., 2003 “Noise, turbulence, and thrust of subsonic freejets from lobed nozzles”, *AIAA Journal*, Vol. 41, No. 3.

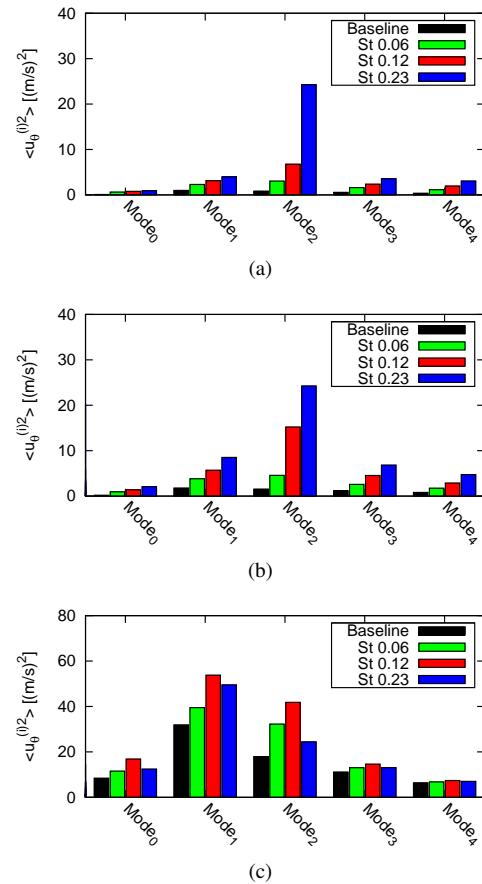


Figure 10: Fluctuation energy of azimuthal modes of azimuthal velocity component at $R=0.25D$ (where peak levels are observed); (a) $x/D = 2.5$; (b) $x/D = 3$; (c) $x/D = 6$.